



## SPECIAL ISSUE PAPER

# Improved performance of inverted polymer solar cells using pentacene

Feng Yang, Eung-Kyu Park, Jae-Hyoung Kim and Yong-Sang Kim<sup>\*,†</sup>

School of Electronic and Electrical Engineering, Sungkyunkwan University, Suwon, Gyeonggi 440-746, Republic of Korea

## SUMMARY

We investigated the role of pentacene in inverted polymer solar cells based on the blends of poly(3-hexylthiophene) (P3HT), (6,6)-phenyl C<sub>61</sub>-butyric acid methyl ester (PCBM), and pentacene. The performance of organic solar cells with pentacene improved in terms of power conversion efficiency (PCE), thermal stability, and lifetime in the ambient air. The pentacene in the P3HT:PCBM blends modified the crystallization of P3HT and PCBM. The donor–acceptor interface of devices with pentacene was found to be more stable than that without pentacene in the active layer, which was characterized by optical microscopy, atomic force microscopy and ultraviolet–visible absorption spectra. The PCE of pentacene based as-fabricated device was 4.3%, and the PCE of non-encapsulated pentacene device reduced just by about 25% after 4 months. Copyright © 2015 John Wiley & Sons, Ltd.

## KEY WORDS

organic solar cells; inverted polymer solar cells; stability; pentacene

## Correspondence

\*Yong-Sang Kim, School of Electronic and Electrical Engineering, Sungkyunkwan University, Suwon, Gyeonggi 440-746, Republic of Korea.

†E-mail: yongsang@skku.edu

Received 31 March 2015; Revised 17 August 2015; Accepted 12 September 2015

## 1. INTRODUCTION

Polymer solar cells are considered as a future energy technology because of their potential for cost-efficient, lightweight, and flexible applications. Over 10% of power conversion efficiency (PCE) [1] in polymer solar cells has been approached by academic researches [2]. Organic photovoltaics (OPV) evolve in two key factors, that is, efficiency and stability. Inverted polymer solar cells have caught wide attention by their good performance in these two factors [3]. For practical applications, the stability is one of the important aspects of inverted polymer solar cells. Especially in roll-to-roll process, OPV devices are subjected to light, oxygen, and humidity during the fabrication [4]. Roll-to-roll devices usually pass through several oven stages to remove solvents of each layer. The active layer of polymer solar cells, which is composed of a polymer donor and fullerene derivatives acceptor, has the tendency to rapidly coarsen when thermal annealing above its glass transition temperature is performed. The interpenetrating donor–acceptor networks and the phase separation are very sensitive to thermal treatments. Elevated processing and operating temperatures are real challenges to the long-term stability of inverted polymer solar cells before their practical applications.

The glass transition temperature of the acceptor fullerene derivative [6,6]-phenyl-C<sub>61</sub>-butyric acid methyl ester (PCBM) is about 110–140 °C [5,6]. During the thermal annealing process, it is very difficult to fix the phase separation between PCBM and the polymer in the active layer. Fullerene molecules start to slowly aggregate and form micrometer-sized crystals at high annealing temperature [7–9]. The PCE of OPV devices could decrease a lot because of the overgrowth crystallite of PCBM in the active layer [10,11]. Several strategies have been explored to control the phase separation of donor and acceptor. There are many works on cross-linking reactions of the polymer [12,13] or fullerene [14,15] in the active layer. The cross-linked molecules could prevent further coarsening of the polymer and fullerene phases. However, cross-linking reactions require advanced chemical modifications that usually reduce the device performance. On the other hand, by introducing additive molecules into the active layer, such as C<sub>60</sub> [7], PC<sub>71</sub>BM [16], and polymer [17], the crystallization of PCBM can be suppressed to some extent.

Pentacene (Pc) has been involved in organic solar cells and plays an important role in singlet fission process. Singlet fission can dramatically increase the efficiency of organic solar cells by producing two triplet excitons from each absorbed photon [18]. In the system of

pentacene/fullerene bilayer heterojunction, the triplet states ensue from singlet fission in pentacene [19]. The external quantum efficiency above 100% was obtained in singlet-exciton-fission-based pentacene/fullerene device at a portion of the visible spectrum [20]. But, it is demonstrated that single fission competes with the traditional photo-induced electron transfer between pentacene and fullerene [21]. It is a big challenge to find out the ways to efficiently harvest the triplet excitons based on this phenomenon [22]. Therefore, it will be more interesting to introduce pentacene into bulk heterojunction-based polymer solar cells.

The PCBM has been widely used in the polymer solar cells and has many  $\pi$  electrons on its surface. Pentacene also has  $\pi$  electrons on its molecular plane. The  $\pi$ - $\pi$  interaction between the PCBM and pentacene would weaken the interaction of PCBM molecules [23]. This interaction will also modify the interface of polymer:PCBM blend and improve the stability of polymer solar cells. Introduction of pentacene into the active layer would enhance the performance of OPV devices, both in stability and efficiency.

In this study, pentacene was used in the bulk heterojunction of polymer solar cells. We investigated the role of pentacene in inverted devices based on poly(3-hexylthiophene) (P3HT) and PCBM, fabricated by the blends of P3HT:PCBM:Pentacene. The OPV devices were fabricated with the structure of ITO/ZnO/P3HT:PCBM:Pentacene/PEDOT:PSS/Ag (Figure 1). A high thermally stable and long lifetime device in the air was obtained by introducing pentacene into the active layer. The polymer-PCBM interfaces of devices with pentacene were more stable than that without pentacene in the active layer, which was characterized by optical microscopy, atomic force microscopy (AFM) and ultraviolet (UV)-visible absorption spectra. The carrier transport of the active layer was also investigated. The long-term stability of non-encapsulated inverted devices is discussed in details.

## 2. EXPERIMENT DETAILS

Poly(3-hexylthiophene) was purchased from Rieke Metals (Lincoln, NE, USA) and PCBM from Nano-C (Westwood,

MA, USA). Pentacene was purchased from Polysis Pure Products, Co. (Seoul, Korea). PEDOT:PSS (ICP 1020) was supplied by Agfa Indusries Korea Ltd. (Seoul, Korea). The indium tin oxide (ITO)-coated glass was supplied by Fine Chemicals (Busan, Korea) ( $15\ \Omega$  per square sheet resistance and 0.7 mm thickness). Anhydrous chlorobenzene (99.9%) was from Sigma Aldrich (St. Louis, MO, USA). Triton X-100, extra pure, was supplied by Do Chemical Co., Ltd. (Seoul, Korea). Hexamethyldisilazane was purchased from AZ Electronic Materials (Singapore, Singapore).

The fabrication and characterization of the devices are as follows. The ITO substrates were ultra-sonicated twice for 10 min in deionized water followed by acetone and then isopropyl alcohol. A filtered ZnO precursor solution was spun cast onto cleaned ITO substrates and then baked in an oven at 200 °C for 20 min [24]. By this way, a ZnO film of 40 nm was obtained on the ITO substrate. A 1:1: $x$  ( $x=0, 0.1, 0.2, 0.3$ ) w/w blend of P3HT, PCBM, and pentacene, with the concentration of 20 mg/mL for P3HT, was dissolved in chlorobenzene by ultrasonication of 3 h, filtered through a 0.45- $\mu$ m PVDF filter, and spun cast on the ZnO-coated ITO substrates. The formed active layer of P3HT:PCBM:Pentacene was 120–130 nm in thickness. In order to deposit hydrophilic PEDOT:PSS on hydrophobic active layer, PEDOT:PSS was modified with 0.5% v/v of Triton X-100 nonionic surfactant. Also, hexamethyldisilazane was first spin-coated on the active layer, followed by the PEDOT:PSS deposition [25]. The modified solution of PEDOT:PSS was spin-coated on the active layer. The film substrates were annealed in an oven at 160 °C for 10 min. A PEDOT:PSS film of 30–40 nm was obtained on the active layer. The devices were finished for measurement after the thermal deposition of ~100 nm thick silver (Ag) film through a shadow mask. The aging process for devices was carried out on a hot plate at 120 °C for varying times. All fabrication processes were carried out in the ambient air except thermal deposition process of silver. The active area of each device was 0.1 cm<sup>2</sup>. The current density versus voltage ( $J$ - $V$ ) characterization of devices was carried out with  $J$ - $V$  curve tracer (Eko MP-160) and a solar simulator (Yss-E40, Yamashita Denso) under AM

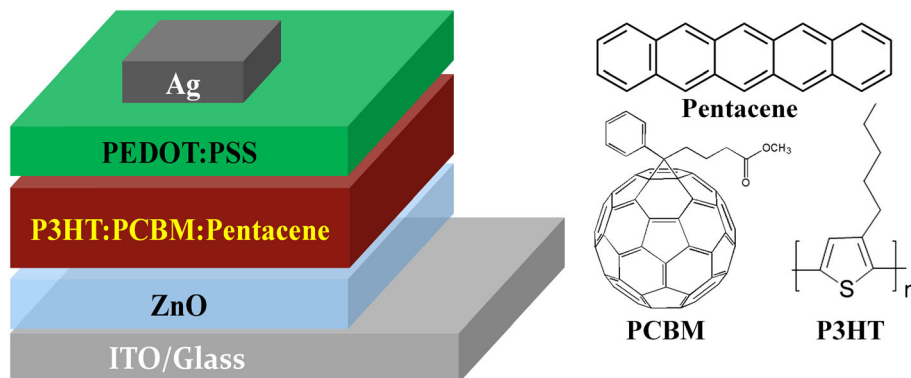


**Figure 1.** Schematic of the inverted polymer solar cell device and the chemical structure of materials in the active layer. PCBM, (6,6)-phenyl C<sub>61</sub>-butyric acid methyl ester; P3HT, poly(3-hexylthiophene); ITO, indium tin oxide.

1.5G irradiation with the intensity of  $100 \text{ mW/cm}^2$ , calibrated by Newport certified standard silicon cell. Absorption spectroscopy measurements were made over a wavelength range from 300 to 1000 nm using a Shimadzu UV-1601 UV-vis spectrophotometer. Optical microscopy images were obtained using an Olympus BX41 Microscope Digital Camera. AFM images were obtained with an advanced scanning probe microscope (PSIA Corp). The thicknesses of all films were characterized by a surface profiler (Tencor Alpha-Step).

### 3. RESULTS AND DISCUSSION

We set out with the hypothesis that the performance of inverted polymer solar cells in terms of stability and efficiency can be enhanced by introducing small molecule pentacene into the active layer. We fabricated the reference devices based on P3HT:PCBM (1:1) blends without the pentacene and the pentacene devices based on the blends of P3HT:PCBM:Pentacene. Several blends of P3HT:PCBM:Pentacene (1:1: $x$ ,  $x=0.1, 0.2, 0.3$ ) were dissolved in chlorobenzene. The corresponding photovoltaic parameters (PCE, open circuit voltage  $V_{OC}$ , short circuit current density  $J_{SC}$ , and fill factor FF) of all the devices are summarized in Table I. In Figure 2, it can be seen that the  $J_{SC}$  and FF of pentacene devices are almost similar as that of reference device. However, the  $V_{OC}$  of pentacene device improved from 0.60 to 0.64 V. As a result, the PCE of 4.3% was achieved from pentacene devices, which is higher than that of reference device.

The morphological effect of pentacene on the active layer was further studied, as shown in Figure 3. We deposited the active layer of reference and pentacene devices on the ZnO/ITO glass substrates followed by the PEDOT:PSS deposition. Figure 3 shows the optical microscopy image of OPV devices (without Ag electrode), after thermally annealing in an oven at  $160^\circ\text{C}$  for 10 min. The optical microscopy images of these active layers show a clear difference in morphology between the reference device and pentacene device. There are many crystallites of PCBM on the surface of the active layer (P3HT:PCBM blend) in reference devices after thermal treatment. The length of PCBM crystallites in the active layer was about  $20 \mu\text{m}$ . However, the surfaces of the active layer (P3HT:PCBM:Pentacene blend) in pentacene devices are very clean without any crystallite of PCBM.

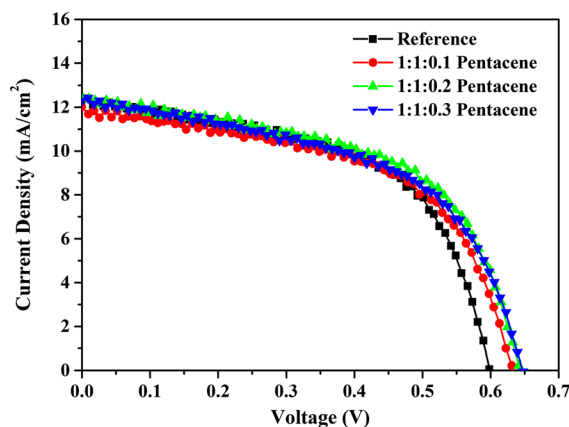


**Figure 2.** Current density–voltage characteristics of reference and pentacene devices under illumination of AM 1.5G,  $100 \text{ mW/cm}^2$ .

Pentacene was found to effectively suppress the micrometer-sized crystallization of PCBM in the active layer (see Figure S1 in the Supporting Information). We hypothesized that the addition of pentacene to the P3HT:PCBM blend controls the growth kinetics of PCBM crystallites such that the crystal overgrowth of PCBM in micrometer size disappeared off the active layer. Therefore, the morphological thermal stability of OPV devices with pentacene was enhanced.

In order to further investigate the morphological effect of pentacene on the active layers, AFM characterization was performed. In Figure 4, the donor–acceptor phase separation of active layer with pentacene was more stable after thermal treatment at  $160^\circ\text{C}$  for 10 min (Figure 4(b)). The interface of donor grains and acceptor grains was clearer than those of reference device. However, the root mean square roughness ( $\sigma_{rms}$ ) of pentacene device was 7.95 nm, a little larger than the  $\sigma_{rms}$  of reference device without pentacene, 7.48 nm. The increase in  $\sigma_{rms}$  of pentacene devices indicated that the pentacene highly modified the morphology of the active layer. There are many crystallites of PCBM (see Figure S1–S2 in the Supporting Information) on the surface of reference active layers, but no crystallite of PCBM on the active layer of pentacene devices was seen. Pentacene devices without PCBM crystallites both in AFM images and optical microscopy images supported that the inclusion of pentacene in the device can enhance the morphology of active layer. It is very effective to improve the thermal stability of OPV device with pentacene.

**Table I.** Photovoltaic parameters of the reference and pentacene devices.

Materials	$J_{SC} [\text{mA/cm}^2]$	$V_{OC} [\text{V}]$	FF	PCE [%]
Reference	12.23 ( $\pm 0.45$ )	0.60 ( $\pm 0.00$ )	0.56 ( $\pm 0.02$ )	4.08 ( $\pm 0.15$ )
1:1:0.1 Pentacene	11.91 ( $\pm 0.24$ )	0.63 ( $\pm 0.00$ )	0.54 ( $\pm 0.01$ )	4.08 ( $\pm 0.13$ )
1:1:0.2 Pentacene	12.31 ( $\pm 0.32$ )	0.64 ( $\pm 0.00$ )	0.55 ( $\pm 0.01$ )	4.30 ( $\pm 0.11$ )
1:1:0.3 Pentacene	12.26 ( $\pm 0.48$ )	0.64 ( $\pm 0.01$ )	0.53 ( $\pm 0.01$ )	4.12 ( $\pm 0.21$ )

FF, fill factor; PCE, power conversion efficiency.  
The values in the brackets represent standard deviation of 20 devices.

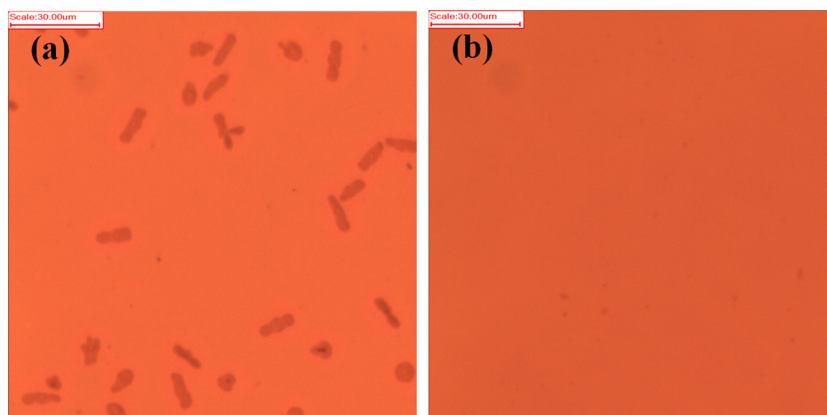


**Figure 3.** Optical microscopy images of (a) reference device (without pentacene) and (b) pentacene device. Scale bar = 30  $\mu\text{m}$ .

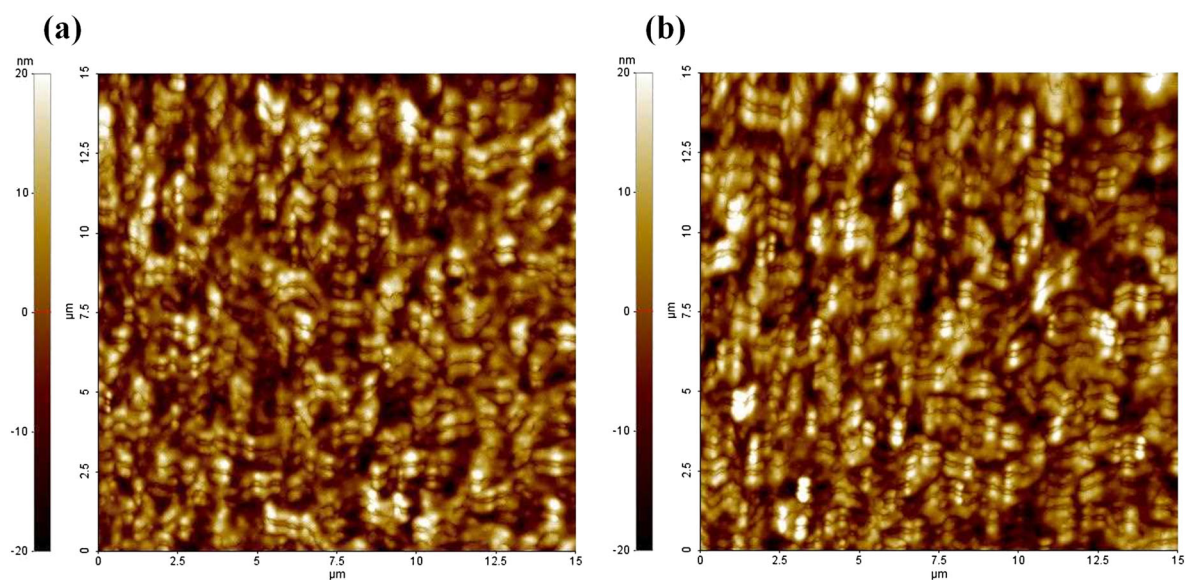


**Figure 4.** Atomic force microscopy topography images of active layers after thermal treatment at 160  $^{\circ}\text{C}$  for 10 min, (a) reference device (without pentacene) and (b) pentacene device.

The effect of pentacene on active layer was also characterized using the UV–visible absorption spectra in Figure 5. The low absorption in the reference device (open square) at a wavelength of 336 nm, the lowest energy absorption feature for PCBM, indicates migration of the isolated PCBM molecules to join large PCBM crystallites [10]. The effect of pentacene on crystallization of PCBM is evident from the active layer before any thermal treatment, which had a higher absorbance at 336 nm (closed square). However, after annealing at 160  $^{\circ}\text{C}$  for 10 min, the absorbance at 400–600 nm in reference device slightly increased (open circle), which represents the absorption region of P3HT, denoting the harvesting of incident light. There are many needle-like crystallites of PCBM on the surface of active layer of the reference device. The thickness of these needle-like crystallites is around 400 nm (see Figure S1–S2 in the Supporting Information). The increase in absorption (especially at 650–700 nm) is expected as these large PCBM

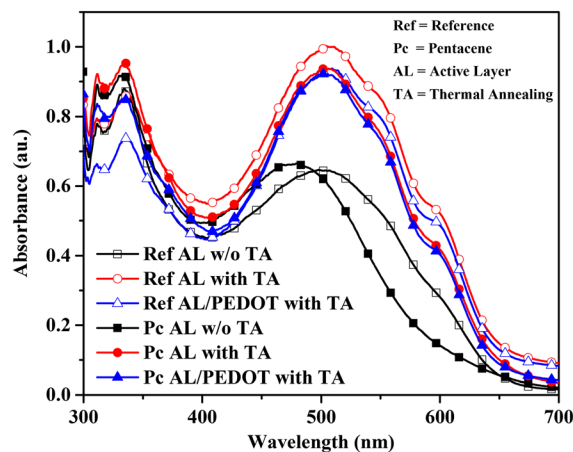


**Figure 5.** Ultraviolet–visible absorption spectra of different layers of organic photovoltaics devices before and after thermal annealing for 10 min at 160  $^{\circ}\text{C}$ .



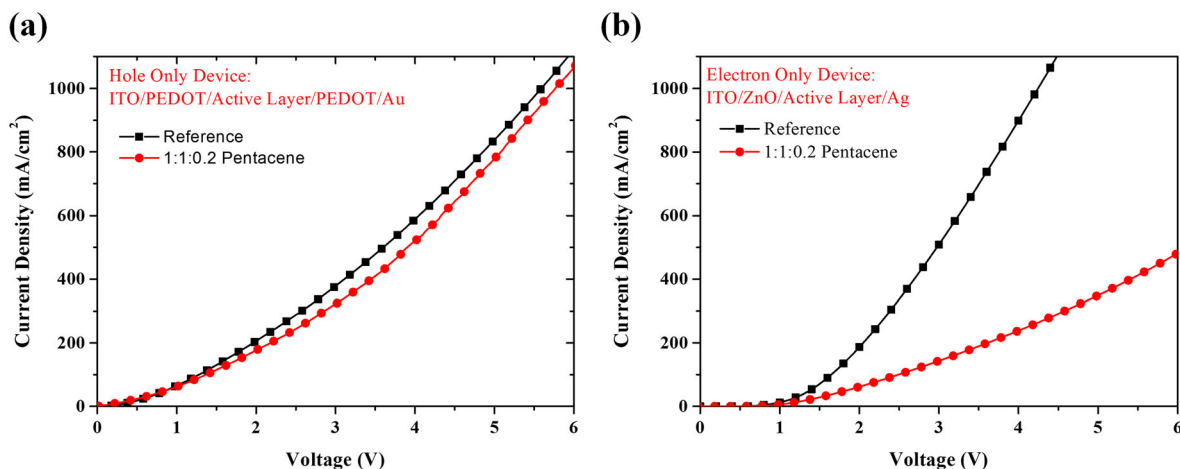


**Figure 6.** J-V characteristics of (a) hole-only devices and (b) electron-only devices, in the dark. ITO, indium tin oxide.

crystallites will confront or scatter the incident light, resulting in higher absorbance background [10].

The absorption of the two complete devices shows almost same properties, except for the two points in pentacene device. The first point is the increase in absorption of pentacene device (solid triangle) at 336 nm compared with the reference device (opened triangle). The increase confirmed that the crystallization of PCBM in pentacene device has been suppressed much. The second point is the decrease in pentacene device at 605 nm, which indicates that the crystallization of P3HT was also suppressed a little. Suppressing the crystallization of P3HT makes the highest occupied molecular orbital deeper [26], which is beneficial for higher  $V_{OC}$ . We imply that both of the two points contribute to the improvement in  $V_{OC}$ . The weak absorbance background of pentacene device after 650 nm will be beneficial to design tandem solar cells in the future. In tandem solar cells, the absorption spectra of whole cell can be expanded by using complimentary donor materials in the two subcells. Pentacene-added front subcell would let more light go through real subcells, which can be beneficial for high PCEs of tandem solar cells [27,28].

To analyze the electrical characteristic of charge transport, we fabricated the hole-only devices with structures of ITO/PEDOT:PSS/Active layer/PEDOT:PSS/Au and electron-only devices of structure ITO/ZnO/Active layer/Ag. As shown in Figure 6(a), the current density of pentacene hole-only device is a little lower than that of the reference. The current density decreased by 10% during hole transport in pentacene device. Meanwhile, the current density of the pentacene electron-only device was much lower than that of the reference, as shown in Figure 6 (b). The low electron transport of the electron-only pentacene device comes from the less surface ratio between crystalline PCBM and silver. The effect of pentacene on the crystallization of PCBM between active layer and silver resulted in lower electron transport. However, the  $J_{SC}$  of pentacene devices is almost the same as the reference device as shown in Table I. We suggest that the  $J_{SC}$  of

pentacene device remained similar because of the single fission process within pentacene. Unfortunately, there is a competition between single fission and traditional photo-induced electron transfer [21]. In the bulk heterojunction, there are many donor-acceptor interface for singlet excitons dissociation and very few chances for singlet fission into two triplet excitons. Therefore, the single fission process could not improve the  $J_{SC}$  much. Nevertheless, organic solar cells with pentacene did not lose the  $J_{SC}$  much and achieved a good PCE.

The thermal stability of inverted polymer solar cells with pentacene was also enhanced. The normalized PCE of pentacene devices as a function of aging time at 120 °C is shown in Figure 7. The PCE of pentacene devices was thermally stable during the aging process while that of reference devices dramatically decreased. The thermal stability increased with increasing pentacene content in the active layer. The 1:1:0.3 pentacene devices showed the best thermal stability.

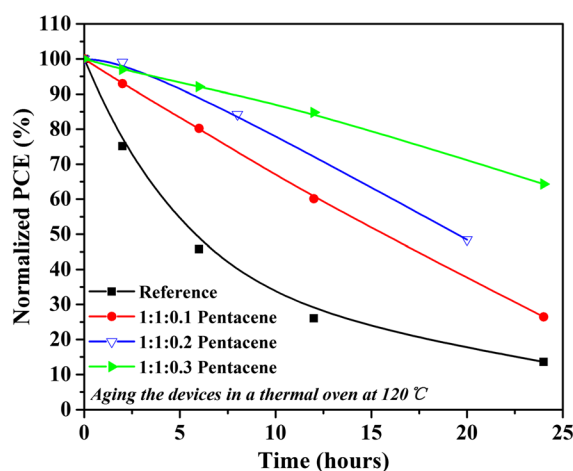


**Figure 7.** Normalized power conversion efficiency (PCE) of reference and pentacene-based organic photovoltaics devices as a function of aging time at 120 °C.

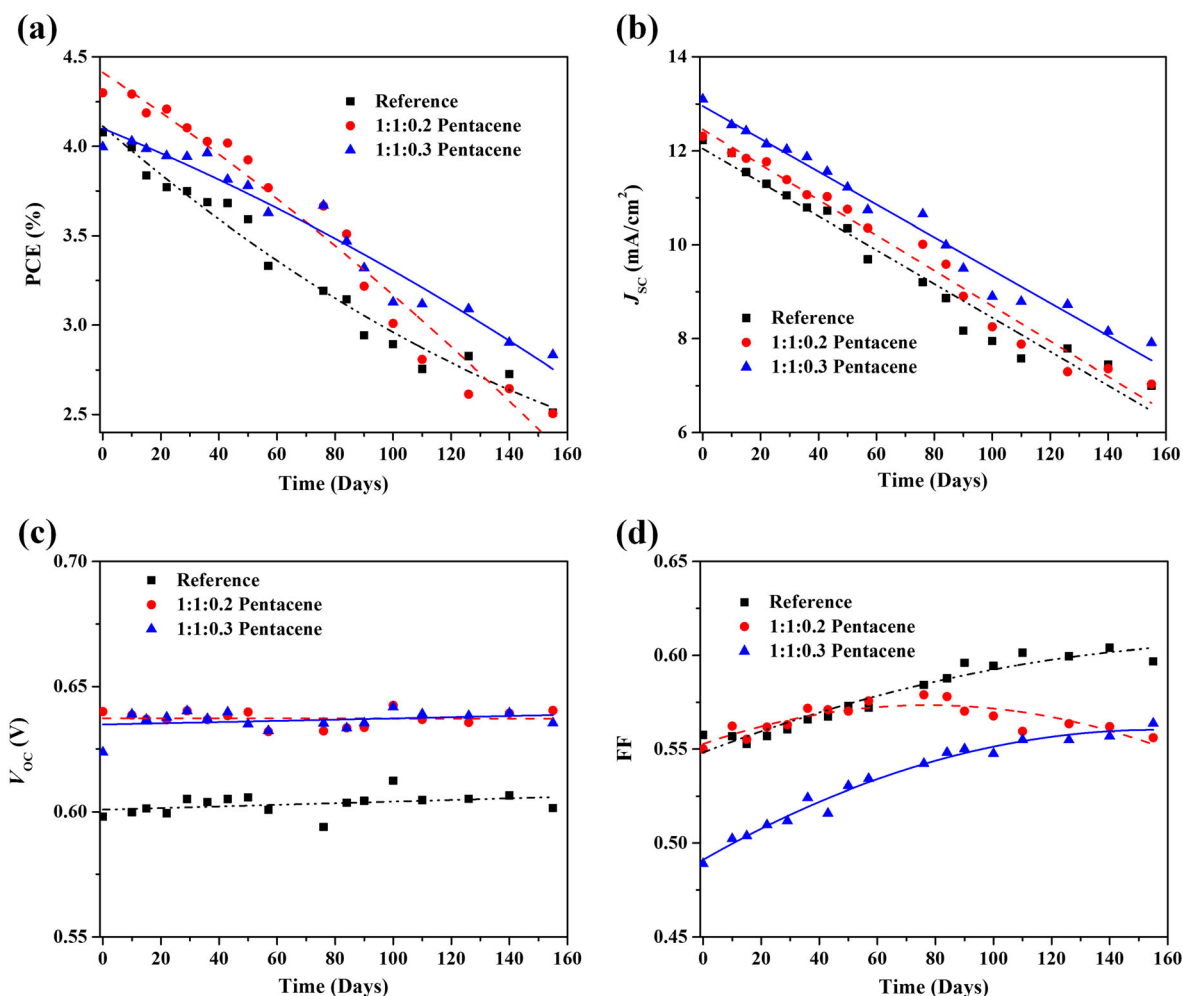


**Figure 8.** Photovoltaic parameter, (a) power conversion efficiency (PCE), (b)  $J_{SC}$ , (c)  $V_{OC}$ , (d) fill factor (FF), of non-encapsulated organic photovoltaics devices based on reference, 1:1:0.2 pentacene and 1:1:0.3 pentacene as a function of time under the air.

We also studied the long-term stability [4,29,30] of non-encapsulated inverted polymer solar cells (four devices for each case). Pentacene devices and reference devices without any encapsulation were kept in ambient air for about 5 months. All the photovoltaic parameters for long-term stability versus time are highlighted in Figure 8(a)–(d). The degradation of PCE and  $J_{SC}$  has the same trend for both pentacene devices and reference devices (Figure 8(a) and (b)). The  $V_{OC}$  was essentially stable for all the devices as shown in Figure 8(c). In Figure 8(d), the FF slightly increased for reference devices and 1:1:0.3 pentacene devices. The PCE of pentacene devices (1:1:0.3) reduced by about 25% within 4 months (see Figure S3 in the Supporting Information). The PCE and  $J_{SC}$  of pentacene devices were higher than those of reference devices during 120 days. However, pentacene is more sensitive to the air compared with P3HT and PCBM. The relatively fast drop in performance of pentacene device (1:1:0.2) after 90 days should come from the degradation of pentacene in the active layer, and the decrease in its FF after 90 days also confirmed this. The pentacene in the active layer seems to

protect the P3HT and PCBM from the air. As a result, the inverted polymer solar cells with pentacene will have a long-term lifetime when encapsulated.

## 4. CONCLUSION

We investigated the role of pentacene in inverted polymer solar cells based on P3HT and PCBM. The pentacene in active layer modified the crystallization of P3HT and PCBM. The donor–accepter interfaces of devices with pentacene were found to be more stable than that without pentacene. A high thermally stable and long lifetime device in ambient air was obtained by introducing pentacene into the active layer. Although both the carrier transport decreased (holes and electrons), the pentacene devices did not lose the  $J_{SC}$  and achieved a good PCE. The PCE of non-encapsulated pentacene device was only reduced by about 25% within 4 months in the ambient air. Overall, the inverted polymer solar cells with pentacene achieved good thermal and long-term lifetime stability without

highly decreasing the efficiency. Based on this work, the organic solar cells could have a better performance and be more possible for mass production.

## ACKNOWLEDGEMENTS

This work was supported under the framework of international cooperation program managed by National Research Foundation of Korea (no. 2014K2A2A2000803) and also supported by the Human Resources Development program (no. 20144030200580) of the Korea Institute of Energy Technology Evaluation and Planning (KETEP) grant funded by the Korea government Ministry of Trade, Industry and Energy.

## REFERENCES

1. You J, Dou L, Hong Z, Li G, Yang Y. Recent trends in polymer tandem solar cells research. *Progress in Polymer Science* 2013; **38**:1909–1928.
2. Chen C, Chang W, Yoshimura K, Ohya K, You J, Gao J, Hong Z, Yang Y. An efficient triple-junction polymer solar cell having a power conversion efficiency exceeding 11%. *Advanced Materials* 2014; **26**:5670–5677.
3. Han D, Yoo S. The stability of normal vs. Inverted organic solar cells under highly damp conditions: comparison with the same interfacial layers. *Solar Energy Materials and Solar Cells* 2014; **128**:41–47.
4. Jorgensen M, Norrman K, Gevorgyan SA, Tromholt T, Andreasen B, Krebs FC. Stability of polymer solar cells. *Advanced Materials* 2012; **24**:580–612.
5. Moule AJ, Meerholz K. Controlling morphology in polymer–fullerene mixtures. *Advanced Materials* 2008; **20**:240–245.
6. Bavel SSV, Sourty E, With DG, Loos J. Three-dimensional nanoscale organization of bulk heterojunction polymer solar cells. *Nano Letters* 2009; **9**:507–513.
7. Lindqvist C, Bergqvist J, Feng C, Gustafsson S, Backe O, Treat ND, Bounioux C, Henriksson P, Kroon R, Wang E, Velasco AS, Kristiansen PM, Stingelin N, Olsson E, Inganäs O, Andersson MR, Müller C. Fullerene nucleating agents: a route towards thermally stable photovoltaic blends. *Advanced Energy Materials* 2014; **4**:1301437.
8. Bertho S, Janssen G, Cleij TJ, Conings B, Moons W, Gradisa A, Dhaen J, Goovaerts E, Lutsen L, Manca J, Vanderzande D. Effect of temperature on the morphological and photovoltaic stability of bulk heterojunction polymer: fullerene solar cells. *Solar Energy Materials & Solar Cells* 2008; **92**:753–760.
9. Kesters J, Kudret S, Bertho S, Brande NV, Defour M, Mele BV, Penxten H, Lutsen L, Manca J, Vanderzande D, Maes W. Enhanced intrinsic stability of the bulk heterojunction active layer blend of polymer solar cells by varying the polymer side chain pattern. *Organic Electronics* 2014; **15**:549–562.
10. Richards JJ, Rice AH, Nelson RD, Kim FS, Jenekhe SA, Luscombe CK, Pozzo DC. Modification of PCBM crystallization via incorporation of C<sub>60</sub> in polymer/fullerene solar cells. *Advanced Functional Materials* 2013; **23**:514–522.
11. Wong HC, Li Z, Tan CH, Zhong H, Huang Z, Bronstein H, McCulloch I, Carbral JT, Durrant JR. Morphological stability and performance of polymer–fullerene solar cells under thermal stress: the impact of photoinduced PC<sub>60</sub>BM oligomerization. *ACS NANO* 2014; **8**:1297–1308.
12. Kim HJ, Han AR, Cho CH, Kang H, Cho HH, Lee MY, Frechet JMJ, Oh JH, Kim BJ. Solvent-resistant organic transistors and thermally stable organic photovoltaics based on cross-linkable conjugated polymers. *Chemistry of Materials* 2012; **24**:215–221.
13. Nam CY, Qin Y, Park YS, Hlaing H, Lu X, Ocko BM, Black CT, Grubbs RB. Photo-cross-linkable azide-functionalized polythiophene for thermally stable bulk heterojunction solar cells. *Macromolecules* 2012; **45**:2338–2347.
14. Hsieh CH, Cheng YJ, Li PJ, Chen CH, Dubosc M, Liang RM, Hsu CS. Highly efficient and stable inverted polymer solar cells integrated with a cross-linked fullerene material as an interlayer. *Journal of the American Chemical Society* 2010; **132**:4887–4893.
15. Diacon A, Derue L, Lecourtier C, Dartel O, Wantz G, Hudhomme P. Cross-linkable azido C<sub>60</sub>-fullerene derivatives for efficient thermal stabilization of polymer bulk-heterojunction solar cells. *Journal of Materials Chemistry C* 2014; **2**:7163–7167.
16. Lindqvist C, Bergqvist J, Bache O, Gustafsson S, Wang E, Olsson E, Inganäs O, Andersson MR, Müller C. Fullerene mixtures enhance the thermal stability of a non-crystalline polymer solar cell blend. *Applied Physics Letters* 2014; **104**:153301.
17. Zheng L, Liu J, Sun Y, Ding Y, and Han Y. Manipulating the crystallization of methanofullerene thin films with polymer additives. *Macromolecular Chemistry and Physics* 2012; **213**: 2081–2090.
18. Zimmerman PM, Bell F, Casanova D, Head-Gordon M. Mechanism for singlet fission in pentacene and tetracene: from single exciton to two triplets. *Journal of the American Chemical Society* 2011; **133**:19944–19952.
19. Chan WL, Ligges M, Jailaubekov A, Kaake L, Miaja-Avila L, Zhu XY. Observing the multiexciton state in singlet fission and ensuing ultrafast multielectron transfer. *Science* 2011; **334**:1541–1545.

20. Congreve DN, Lee J, Thompson NJ, Hontz E, Yost SR, Reuswig PD, Bahlke ME, Reineke S, Voorhis TV, Baldo MA. External quantum efficiency above 100% in a singlet-exciton-fission-based organic photovoltaic cell. *Science* 2013; **340**:334.
21. Akimov AV, Prezhdov OV. Nonadiabatic dynamics of charge transfer and singlet fission at the pentacene/C<sub>60</sub> interface. *Journal of the American Chemical Society* 2014; **136**:1599–1608.
22. Piland GB, Burdett JJ, Dillon RJ, Bardeen CJ. Singlet fission: from coherences to kinetics. *The Journal of Physical Chemistry Letters* 2014; **5**:2312–2319.
23. Yang F, Kim J-H, Ge Z, and Kim Y-S. Enhanced thermal stability of inverted polymer solar cells with pentacene. *Israel Journal of Chemistry* 2015; DIO: 10.1002/ijch.201400212.
24. Park E-K, Kim J-H, Kim J-H, Park M-H, Lee D-H, Kim Y-S. Dissimilar mechanism of executing hole transfer by WO<sub>3</sub> and MoO<sub>3</sub> nanoparticles in organic solar cells. *Thin Solid Films* 2015; **587**:137–141.
25. Baek W-H, Choi M, Yoon T-S, Lee HH, Kim Y-S. Use of fluorine-doped tin oxide instead of indium tin oxide in highly efficient air-fabricated inverted polymer solar cells. *Applied Physics Letter* 2010; **96**:133506.
26. Tsoi WC, Spencer SJ, Yang L, Ballantyne AM, Nicholson PG, Turnbull A, Shard AG, Murphy CE, Bradley DDC, Nelson J, Kim JS. Effect of crystallization on the electronic energy levels and thin film morphology of P3HT:PCBM blends. *Macromolecules* 2011; **44**:2944–2952.
27. Kouijzer S, Esiner S, Frijters CH, Turbiez M, Wienk MM, Janssen RAJ. Efficient inverted tandem polymer solar cells with a solution-processed recombination layer. *Advanced Energy Materials* 2012; **2**:945–949.
28. Ameri T, Li N, Brabec CJ. Highly efficient organic tandem solar cells: a follow up review. *Energy Environmental Science* 2013; **6**:2390–2413.
29. Zimmermann B, Wurfel u, Niggemann M. Longterm stability of efficient inverted P3HT:PCBM solar cells. *Solar Energy Materials & Solar Cells* 2009; **93**:491–496.
30. Dai A, Wan A, Magee C, Zhang Y, Barlow S, Marder SR, Kahn A. Investigation of p-dopant diffusion in polymer films and bulk heterojunctions: stable spatially-confined doping for all-solution processed solar cells. *Organic Electronics* 2015; **23**:151–157.

## SUPPORTING INFORMATION

Additional supporting information may be found in the online version of this article at the publisher's web site.